Adventures on the Interface of Mechanics and Control

Edited by
K. Alfriend, M. Akella, J. Hurtado,
J. Juang and J. Turner

Tech Science Press
www.techscience.com

HIGH ACCURACY TRAJECTORY AND UNCERTAINTY PROPAGATION ALGORITHM FOR LONG-TERM ASTEROID MOTION PREDICTION

James D. Turner[1]   Tarek Elgohary[2]   Manoranjan Majji[3]

John L. Junkins[4]

ABSTRACT

Asteroid mitigation strategies fundamentally depend on understanding accurate predictions for the asteroid motion as it approaches the neighborhood of the Earth. Accurate calculations require multi-year estimates for the object's trajectory. Equally important, however, one needs uncertainty envelope predictions that bound the expected range of variability in the time of arrival and proximity to the Earth. Hundreds of papers have investigated algorithms for ensuring that highly accurate motion predictions are generated. Because the fundamental equations are nonlinear, a repeated sampling of the system acceleration solution is invoked in order to predict the expected range in variability in the asteroid's position and velocity at future times. Examples of this approach include predictor-corrector and Runge-Kutta methods where many samples are combined to provide a weighted approximation for the motion predictions. Classically it has proved to be difficult to derive and code high order models for the two-body accelerations. The main contribution of this paper is the demonstration that by defining Lagrange-like invariants easily derived analytical models are developed for exactly computing the two-body accelerations to arbitrary order. With arbitrary order time derivatives available, it is further shown that one can develop a rigorous analytical Taylor series based solution for

---

[1] Aerospace Engineering, Texas A&M University, College Station, Texas, turner@aero.tamu.edu

[2] Aerospace Engineering, Texas A&M University, College Station, Texas

[3] Mechanical& Aerospace Engineering, U at Buffalo Buffalo-NY-14260

[4] Aerospace Engineering, Texas A&M University, College Station, Texas

propagating the position and velocity vectors for the nonlinear two-body problem. The key algorithmic innovation is the recognition that the proposed Lagrange-like invariants can differentiated to arbitrary order by using the well known Leibniz product rule. Several numerical examples are presented to demonstrate the effectiveness of the proposed algorithmic solutions.

1. INTRODUCTION

The two-body equations of motion are integrated by evaluating an analytical Taylor series, where exact arbitrary order time derivatives of the acceleration equations are computed. The time derivative models are developed by introducing Lagrange-like invariants that are easily differentiated by invoking Leibnitz product rule. As with any series-based approximation there remains an open question regarding the convergence of the approximation. Numerical evidence is presented that demonstrates that the proposed series approximations allow large integration step sizes and maintains high accuracy. In deed extended precision calculations have generated solutions that are accurate hundreds of digits. Both the classical Keplerian two-body and perturbed acceleration force models are readily handled [1,7] where the numerical solution for each derivative order is accurate to the working precision of the machine.

Classically the generation of arbitrary order time derivative models has been hindered by the complexity associated with handling fractional powers of complex vector-valued arguments. This complexity barrier is overcome by introducing two scalar Lagrange-like invariant [1,4] (i.e., $f = \mathbf{r}.\mathbf{r}$) and the transformation of the scalar variable $g = f^{-n/2}$ into a differential equation where all fraction terms are eliminated, where time is the independent variable. Leibniz product rule is directly applied to f, where the product is the vector dot product. After developing the first order differential equation for g Leibniz product rule is again invoked to recursively generate the composite function rates for $f, \dot{f} \ddot{f}, \ldots$ and $g, \dot{g}, \ddot{g}, \ldots$. With recursive solutions available for f and g one can recursively generate vector solutions for $\mathbf{r}, \dot{\mathbf{r}}, \ddot{\mathbf{r}}, \cdots$ for arbitrary order. Higher-order gravity perturbations are easily handled.

With the generation of the position and velocity vectors handled by highly accurate

series approximations, the next issue is concerned with investigating the expected range in the uncertainty associated with the initial conditions. To this end, the two-body trajectory uncertainty is handled by generating nonlinear state transition tensors for propagating the initial condition uncertainty in the integrated system response. This approach samples an initial covariance and propagates the variations to the desired future time. The system statistics are recovered by introducing a nonlinear transformation for mapping the evolved initial condition uncertainty into expected variations in the mean motion and motion covariance matrix. The solution for the instantaneous system statistics is mechanized by introducing a high-order vector reversion of series for the tensor-based state transition model for the initial condition uncertainties. The resulting solution effectively solves the *stochastic Liouville equation* for the probability density of the solution along the motion trajectory in presence of low diffusion effects. Two major contributions are presented in the paper: (1) arbitrary order analytic time derivatives for the two-body problem, and (2) an uncertainty propagation method for developing a probability density function that accounts for the non-Gaussian behavior resulting from the systems nonlinear math model.

Data Structures: All of the algorithms to be developed require high-order derivative models. Computationally high order derivative models are analyzed by defining vector-valued n-tuple data structures of the form

$$v := \left(v \quad v' \quad v'' \quad \cdots \quad v^{(n)} \right)$$

where the dimensions of v are dim(v) =(3,0:n), leading to $v = v(:,0)$, $v' = v(:,1)$, and so on. N-tuple data structures greatly simplify the Leibnitz product rule based derivative calculations that follow.

1.1. Nonlinear Differential Equations

Unperturbed Keplerian motion is governed by an inverse square gravity field. For object motions near Earth the equation of motion is defined by[1,4,7]

$$\ddot{\mathbf{r}} = -\mu \mathbf{r} / (\mathbf{r}.\mathbf{r})^{3/2} \tag{1}$$

where $\mathbf{r} = \begin{bmatrix} x, & y, & z \end{bmatrix}$ denotes the inertial relative coordinate vector that locates an object relative to the Earth and $\mu = 398601.2$ km^2/sec^3 is the gravitational con-

stant. Of course asteroid motion applications will involve motions relative to the Sun and other planets; nevertheless, the methodology presented here will generalize for computationally handling these more complicated application domains.

Two Lagrange-Like Invariants: Two scalar quantities are required for automating the generation of arbitrary order time derivatives for the equation of motion. The first Lagrange invariant-like variable[1] is defined by the dot product of the position vector with itself, yielding

$$f = r.r \tag{2}$$

The *n-th* order time derivative of f is computed by evaluating Leibniz's product rule

$$f^{(n)} = \sum_{m=0}^{n} \binom{n}{m} r^{(m)}.r^{(n-m)} \tag{3}$$

where $r^{(m)} = \frac{d^m r}{dt^m}$ and $\binom{n}{m}$ denotes the standard binomial coefficient. This calculation is very straightforward. When using this equation one must be aware that this calculation requires that $r, \dot{r}, \ddot{r}, \cdots, r^{(n)}$ are all available before $f^{(n)}$ can be computed, which suggests that a sequential process is required to processing all required sensitivity terms. The second scalar variable consists of f raised to a fractional power

$$g = (f)^{-p/2} \tag{4}$$

where p denotes the power. The variable p is kept general because perturbation terms require several values for p for analyzing high-order harmonic gravity terms. The classical approach for evaluating time derivatives for Eq. (4) leads to composite function calculations that are handled by introducing the celebrated formula of Faá di Bruno.

Faá di Bruno's Mathematical Identity:The problem of computing composite function derivatives has existed since the earliest days of the invention of calculus. Faá di Bruno addressed this problem in a very general way, in 1857, where he presented a mathematical identity for generalizing the chain rule of calculus to n^{th} order

derivative calculations. His formula for the nth derivative of a function $u = \phi(y)$, where $y = \psi(x)$, is written as

$$\frac{d^n}{dx^n}\phi\left(\psi\left(x\right)\right) = \sum \frac{n!}{b_1!b_2!\cdots b_n!}\phi^{(k)}\left(\psi\left(x\right)\right)\left(\frac{\psi'}{1}\right)^{b_1}$$

$$\left(\frac{\psi''}{1\cdot 2}\right)^{b_2}\left(\frac{\psi'''}{1\cdot 2\cdot 3}\right)^{b_3}\cdots\left(\frac{\psi^{(n)}}{1\cdot 2\cdots n}\right)^{b_m} \quad (5)$$

where $\varphi(y)$ and $\psi(x)$ are assumed to have a sufficient number of derivatives, and the summation extends over all the positive integer solutions of the constraint equations

$$\begin{aligned}
b_1 + b_2 + b_3 + \cdots + b_n &= k \\
b_1 + 2b_2 + 3b_3 + \cdots + nb_n &= n
\end{aligned} \quad (6)$$

Each term appearing in Eq. (5) is defined by the integer solution to the constraint equations of Eq. (6).

Simplified Model for the Composite Function Derivative: Our goal is to develop a differential equation for g; thereby, avoiding the complexities encountered with having to handle Faá di Bruno's complicated combinatorial equation for high-order composite function calculations. This is accomplished by squaring the equation for g and clearing fractional powers by multiplying by f^p, yielding:

$$f^p g^2 = 1 \quad (7)$$

Differentiating *w.r.t.* time and clearing fractional powers yields the 1st order differential equation for g:

$$f\dot{g} + \frac{p}{2}\dot{f}g = 0 \quad (8)$$

that displays the required product form. Computing the *n-th* order time derivative of this equation, by applying Leibniz's product rule to each term, yields

$$\sum_{m=0}^{n}\binom{n}{m}f^{(m)}g^{(n-m+1)} + \frac{p}{2}\sum_{m=0}^{n}\binom{n}{m}f^{(m+1)}g^{(n-m)} = 0 \quad (9)$$

which implicitly defines $g^{(n+1)}$ (i.e., the highest derivative appearing in the equation for g). Solving this equation for $g^{(n+1)}$ yields the desired solution

$$g^{(n+1)} =$$

$$-\left\{\frac{p}{2}\sum_{m=0}^{n}\binom{n}{m}f^{(m+1)}g^{(n-m)} + \sum_{m=1}^{n}\binom{n}{m}f^{(m)}g^{(n-m+1)}\right\}/f \quad (10)$$

or

$$g^{(n+1)} =$$

$$-\left\{\frac{p}{2}f^{(1)}g^{(n)} + \sum_{m=1}^{n}\binom{n}{m}\left(\frac{p}{2}f^{(m+1)}g^{(n-m)} + f^{(m)}g^{(n-m+1)}\right)\right\}/f$$

where a single summation calculation is required. This calculation requires that $g, \dot{g}, \ddot{g}, \cdots, g^{(n)}$ are all available before $g^{(n+1)}$ can be computed. All time derivatives of f and g are defined by Eqs (3) and (10). Introducing g into the two-body equation of motion leads to

$$\ddot{\mathbf{r}} = -\mu r \mathbf{g}$$

which is in the required product form. Applying Leibniz product rule yields the *nth* order time derivative calculation for the two body acceleration:

$$\mathbf{r}^{(2+n)} = -\mu \sum_{m=0}^{n}\binom{n}{m}r^{(m)}g^{(n-m)} \quad (11)$$

where the position and velocity vectors are assumed to be known. As shown in Figure 1 recursive calculations are generated for third order and above. The calculations are initialized by computing the known position and velocity vectors, evaluating the acceleration vector, computing the first two derivatives for f and g analytically, then all high-order derivatives are recursively evaluated using the simple Leibniz product rule for Eqs. (3), (10), and (11)

$$\mathbf{r}^{(n)}, \quad f^{(n)}, \quad g^{(n)} \quad (12)$$

The calculations enabled by Eqs.(3), (10) and (11) permit an arbitrary order analytic continuation series solutions to be developed for propagating the state trajectories, leading to the state trajectory propagation equation

$$\mathbf{r}(t+h) = \mathbf{r}(t) + \dot{\mathbf{r}}h + \frac{\ddot{\mathbf{r}}h^2}{2!} + \frac{\dddot{\mathbf{r}}h^3}{3!} + \frac{\mathbf{r}^{(4)}h^4}{4!} + \dots \quad (13)$$
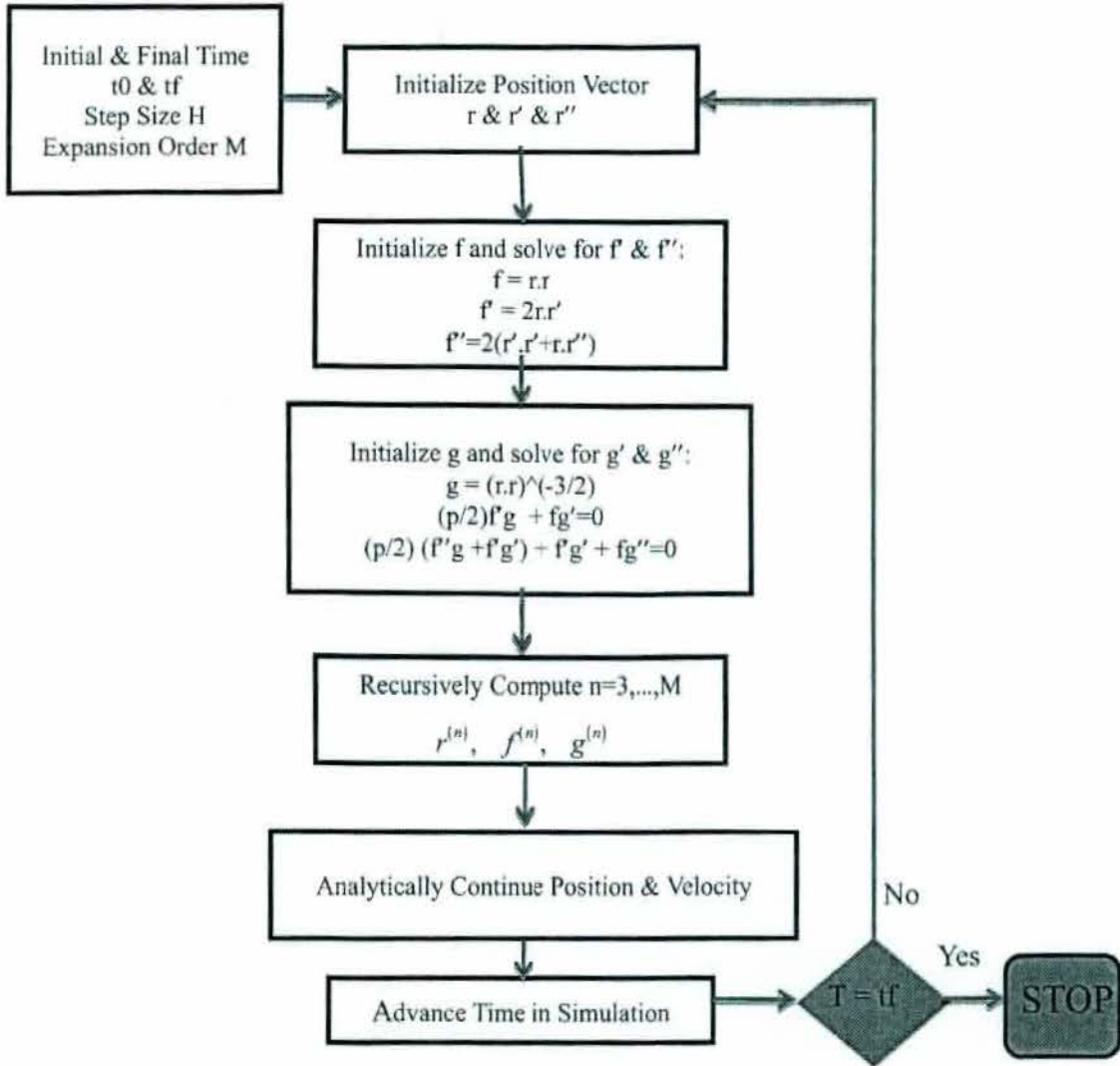
Figure 1: Analytic Continuation Computational Flow Diagram

and the velocity propagation equation

$$\mathbf{v}(t + h) = \dot{\mathbf{r}}(t) + \dot{\mathbf{r}}h + \frac{\ddot{\mathbf{r}}h^2}{2!} + \frac{\mathbf{r}^{(4)}h^3}{3!} + \dots \tag{14}$$

An open question is: how many terms? The resolution of the problem is complicated because the solution accuracy is a function of three variables: (1) number of terms retained, (2) the required accuracy, and (3) the integration step size h. A further complicating factor involves the computer solution accuracy. For example, one open equation is: what is the impact of double precision, quad precision, and/or arbitrary order precision on the number of terms required and the step size for the integration. It is of interest to observe in Table 1 for an orbit where $r = r_{Earth} + 700$

km = 7078 km, how rapidly the derivative terms die off.

The data in Table 1 supports the following conclusions: (1) the derivative values die off rapidly, (2) large integration step sizes require high order expansions (i.e., >7), and (3) algorithms that just sample the acceleration will have a hard time sampling contributions from 9th and higher order terms. Future research will investigate the impact of solution accuracy on the performance of the series approximation. Numerical experiments are performed to establish a 3D trade space between maximum step size and expansion order and solution accuracy.

2. STATE TRANSITION TENSOR MODELS FOR UNCERTAINTY PROPAGATION

With accurate trajectory states available, the next engineering challenge is concerned with generating propagation strategies for the uncertainty that exploits the analyst knowledge of the potential spread in the initial conditions. This problem is addressed by introducing nonlinear state transition tensor models for propagating expected variations in the initial conditions. The governing equations for the first three state transition tensor models orders are given by:

$$
\begin{aligned}
\dot{x} &= f(x, t) \\
\dot{\Phi}_1 &= \nabla f \Phi_1, \quad \Phi_1(t_0, t_0) = I \\
\dot{\Phi}_2 &= \nabla^2 f \Phi_1 \Phi_1 + \nabla f \Phi_2, \quad \Phi_2(t_0, t_0) = 0 \\
\dot{\Phi}_3 &= \nabla^3 f \Phi_1 \Phi_1 \Phi_1 + \nabla^2 f (2\Phi_2 \Phi_1 + \Phi_1 \Phi_2) + \nabla f \Phi_3, \quad \Phi_3(t_0, t_0) = 0
\end{aligned}
\tag{15}
$$

These equations are used to propagate the departures in the conditions form the nominal values for representing the evolution of uncertainty as

$$
\delta x = \Phi_1 \delta x_0 + \frac{1}{2}\Phi_2 \delta x_0 \delta x_0 + \frac{1}{3!}\Phi_3 \delta x_0 \delta x_0 \delta x_0 + \frac{1}{4!}\Phi_4 \delta x_0 \delta x_0 \delta x_0 \delta x_0 + \ldots \tag{16}
$$

where δx_0 denotes a sample perturbation selected from the assumed uncertainty model. To study how the nonlinear system dynamics changes the assumed statistical model for the problem unknowns, Eq. (16) is reverted to provide $\delta x_0 = \delta x_0(\delta x)$. This transformation allows one to compute the mean motion, covariance matrix, and higher order statistical measures, where the reverted series solution is given by:

$$
\delta x_0 = A_1 \delta x + \frac{1}{2}A_2 \delta x \delta x + \frac{1}{3!}A_3 \delta x \delta x \delta x + \frac{1}{4!}A_4 \delta x \delta x \delta x \delta x + \ldots \tag{17}
$$

Table 1: Maximum Derivative value as a function of Expansion Order: Analytic Continuation Computational Flow Diagram

Derivative Order		1	2	3	5	7	10	15	20
Max(R(:,n)) meters	3×10^6	7×10^3	4×10^1	1×10^{-2}	7×10^{-8}	2×10^{-12}	4×10^{-19}	1×10^{-28}	1×10^{-38}

To understand how this equation is used, let us now consider the following change of variables theorem:

Change of Variables: Let $\delta x = g(\delta x_0)$ be an invertible, continuously differentiable mapping, with a differentiable inverse. If the probability density function $p_{\delta x_0}(\delta x_0)$ is known, then the probability density function in the transformed space is given by[8]

$$p_{\delta x}(\delta x) = p_{\delta x_0}\left(\delta x_0 = g^{-1}(\delta x)\right)\left|\det\left(\frac{dg^{-1}(\delta x)}{\delta x}\right)\right|$$

Equation (16) represents a direct transformation (analytic, continuously differentiable, satisfying all conditions stipulated by the change of variables theorem above) between initial conditions and the state at the current time. To this end, once the initial condition distribution is specified, we arrive at an exact expression for the probability density function (*pdf*) at the running time t. The proposed solution effectively solves the *stochastic Liouville* equation for the *pdf* along the motion trajectory. Several numerical examples are provided to validate the state trajectory and uncertainty propagation results.

3. REVERSION OF SERIES SOLUTION FOR THE INITIAL CONDITION UNCERTAINTY

The series expansion for the instantaneous variations in the state perturbation is reverted by introducing Eq. (17) into Eq. (16) and collecting terms. This step leads to the following necessary conditions for inverting the series through *4-th* order:

$$\delta^1 : I = \Phi_1 A_1$$

$$\delta^2 : 0 = \frac{1}{2}\Phi_1 A_2 + \frac{1}{2}\Phi_2 A_1 A_1$$

$$\delta^3 : 0 = \frac{1}{6}\Phi_1 A_3 + \frac{1}{4}\Phi_2(A_1 A_2 + A_2 A_1) + \frac{1}{6}\Phi_3 A_1 A_1 A_1 \tag{18}$$

$$\delta^4 : 0 = \frac{1}{24}\Phi_1 A_4 + \frac{\Phi_2}{4}\left(\frac{1}{3}(A_1 A_3 + A_3 A_1) + 2A_2 A_2\right)$$

$$+ \frac{\Phi_3}{12}(A_1 A_1 A_2 + A_1 A_2 A_1 + A_2 A_1 A_1) + \frac{1}{24}\Phi_4 A_1 A_1 A_1 A_1$$

yielding the tensor coefficient solutions

$$A_1 = \Phi_1^{-1}$$
$$A_2 = -\Phi_1^{-1}\Phi_2 A_1 A_1$$
$$A_3 = -\Phi_1^{-1}\left(\frac{3}{2}\Phi_2\left(A_1 A_2 + A_2 A_1\right) + \Phi_3 A_1 A_1 A_1\right)$$
$$A_4 = -\Phi_1^{-1}\left\{6\Phi_2\left(\frac{1}{3}\left(A_1 A_3 + A_3 A_1\right) + 2A_2 A_2\right)\right.$$
$$\left. + 2\Phi_3\left(A_1 A_1 A_2 + A_1 A_2 A_1 + A_2 A_1 A_1\right) + \Phi_4 A_1 A_1 A_1 A_1\right\} \tag{19}$$

In every case one only needs the first-order state transition matrix to be inverted to recover the series expansion coefficients. It is understood that these operations represent implied tensor contraction operations, since the resulting object sizes vary during the calculations. The series tensor coefficients enable the calculation of the reverted uncertainty propagation equation defined by Eq. (17), where the inverse transformation for the mapping is given by

$$g^{-1}\{\delta x\} = A_1 \delta x + \frac{1}{2}A_2 \delta x \delta x + \frac{1}{3!}A_3 \delta x \delta x \delta x + \frac{1}{4!}A_4 \delta x \delta x \delta x \delta x + ... \tag{20}$$

and the differentiable inverse follows as

$$\frac{dg^{-1}(\delta x)}{d(\delta x)} = A_1 + A_2 \delta x + \frac{1}{2!}A_3 \delta x \delta x + \frac{1}{3!}A_4 \delta x \delta x \delta x + ... \tag{21}$$

The results of applying Eqs. (19) through (21) completely define the *pdf*, which enables fully nonlinear predictions for the mean, covariance, and higher-order statistical moments. Analytically, the tensor coefficients can be interpreted as inverse state transition tensors for mapping the final states to the initial time.

4. INITIAL AND TRANSFORMED PROBABILITY DISTRIBUTION FUNCTION

We assume for the moment the initial multivariate normal distribution is defined by

$$N \sim N\left(\mu, \ \Sigma\right) \tag{22}$$

where $\mu \in \Re^6$ denotes the mean and $\sum$ denotes the covariance matrix. The initial *pdf* is assumed to be given by

$$p\left(\delta x\left(t_0\right)\right) = (2\pi)^{-3} \left|\det \sum\right|^{-\frac{1}{2}} e^{-\frac{1}{2}\left(\delta x(t_0)\right)^T \sum^{-1}\left(\delta x(t_0)\right)} \tag{23}$$

The desired nonlinear *pdf* is then given by

$$p_{\delta x}\left(\delta x\right) = p_{\delta x_0}\left(\delta x_0 = g^{-1}\left(\delta x\right)\right) \left|\det\left(\frac{dg^{-1}\left(\delta x\right)}{\delta x}\right)\right|$$

where g^{-1} and $\frac{dg^{-1}(\delta x)}{d(\delta x)}$ are defined by Eqs. (20) and (21)[8]. This solution effectively solves the *stochastic Liouville* equation for the *pdf* of the solution along the motion trajectory.

5. NUMERICAL RESULTS

The Flow Diagram for the Analytic Continuation is presented in Figure 1. One provides the initial position and velocity vectors, time interval for the simulation, the derivative expansion order, and the number of continuation steps. The recursion works by updating position and velocity, computing f, f', f'', and g, g', g'' and then looping recursively for generating the higher derivatives for f, g, and **r**. The simulation continues until the final propagated final time is reached and the simulation is stopped. The analytic continuation solution for the position and velocity vectors is tested by computing a single orbit, where the initial conditions must be recovered for an accurate solution. Several LEO examples are presented for an initial 7000 km orbit where the following eccentricities 0.05, 0.2, and 0.9 are assumed. The first three cases assume that the motion is in a 2D plane. A fourth LEO example is presented where a 3D motion exists for 0.53 eccentricity orbit. The last example is a circular GEO orbit. In all cases the integration step size has been held fixed. Future research will investigate variable step size algorithms for propagating the position and velocity estimates, which is very important for the asteroid application. For example, the 0.9 eccentricity orbit considered yields minor-level precision in the position estimates after 5000 continuation steps. Nevertheless, very large variations in the allowed continuation step size are theoretically possible, and important when simultaneously propagating the state and transition tensors for uncertainty analysis.

5.1. Case 1: 700 km E = 0.05 elliptical Earth Orbit

The initial position and velocity vectors are

$$r(t_0) = \begin{pmatrix} 7.0 \\ 0.0 \\ 0.0 \end{pmatrix} \times 10^6 m; \qquad \dot{r}(t_0) = \begin{pmatrix} 0.0 \\ 7732.411008 \\ 0.0 \end{pmatrix} \times 10^3 m/\sec \qquad (24)$$

The orbit eccentricity is 0.05. Sub-meter accuracy is achieved for a step size of $\sim$ 629 sec. As the integration step size approaches 300 sec. the solution accuracy is beyond double precision arithmetic (i.e., 14 digits) and only seven series terms are required. Table 2 shows the effect of changing number of steps & number of Series Teams on integration accuracy.

Table 2: Case 1 Elliptical Orbit (E=0.05) Integration Performance & Accuracy Study: Continuation vs. F&G (1 orbit)

# of Continuation Steps & Integration Step Size(sec)(Orbit Period = 6294.6595 sec)	# Series Terms for mm error /Final Integration accuracy
200, 31.4733	4 (10^{-7} m, 10^{-11} m/s)
100, 62.9466	5 (10^{-7} m, 10^{-10} m/s)
80, 78.6832	6 (10^{-8} m, 10^{-11} m/s)
60, 104.9109	6 (10^{-8} m, 10^{-11} m/s)
40, 157.3665	6 (10^{-8} m, 10^{-11} m/s)
3, 209.8220	7 (10^{-7} m, 10^{-10} m/s)
20, 314.7329	8 (10^{-6} m, 10^{-9} m/s)
15, 419.6439	8 (10^{-4} m, 10^{-8} m/s)
10, 629.4660	12 (10^{-2} m, 10^{-6} m/s)
8, 786.8324	15 (10^{1} m, 10^{-3} m/s)

The above results are verified by comparing the continuation solution with the classical F&G solution at each time step. Figure 2 shows the comparison between F&G Series vs continuation solution of each time step using 15 continuation steps with a step size of 419.64 seconds for a complete orbital period. Figure 3 shows orbital period with the association continuation steps.

5.2. Case 2: 7000 km E = 0.2 Elliptical Earth Orbit

The initial position and velocity vectors are

$$r(t_0) = \begin{pmatrix} 7.0 \\ 0.0 \\ 0.0 \end{pmatrix} \times 10^6 m; \qquad \dot{r}(t_0) = \begin{pmatrix} 0.0 \\ 8266.295076 \\ 0.0 \end{pmatrix} \times 10^3 m/\sec \qquad (25)$$

The orbit eccentricity is 0.2. As shown in Table 3, sub-meter accuracy is achieved for a step size of ~ 407 sec. As the integration step size approaches 20 sec. the solution accuracy is beyond double precision arithmetic (i.e., 14 digits) and only seven series terms are required.
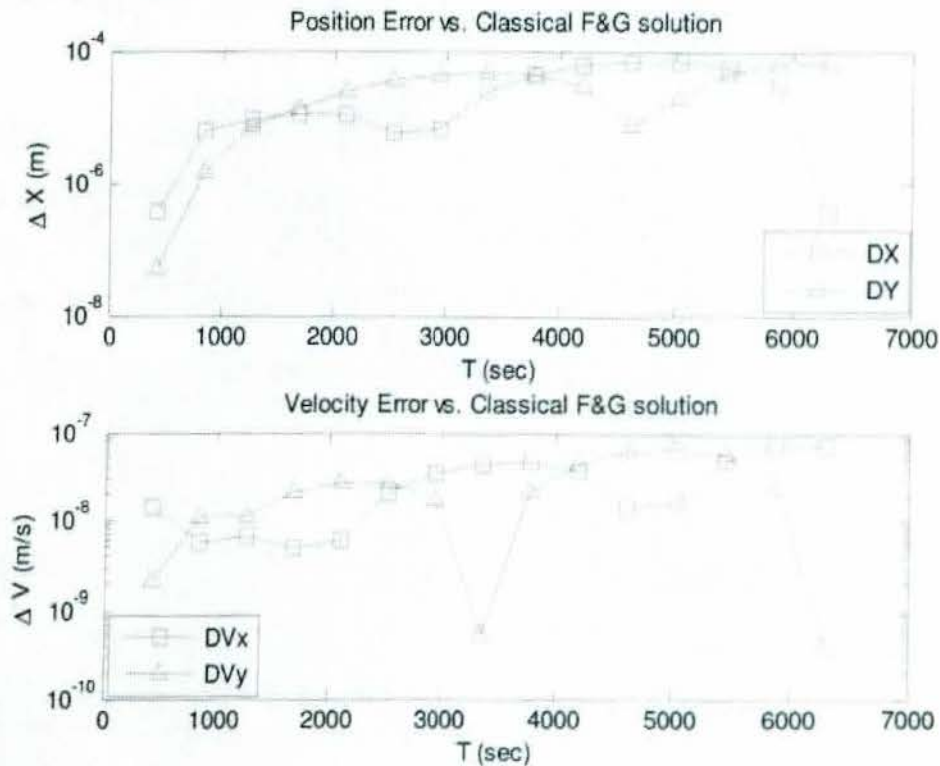

Figure 2: Continuation vs. F&G (1 orbit)

5.3. Case 3: 7000 km E = 0.9 elliptical Earth Orbit

The initial position and velocity vectors are

$$r(t_0) = \begin{pmatrix} 7.0 \\ 0.0 \\ 0.0 \end{pmatrix} \times 10^6 m; \qquad \dot{r}(t_0) = \begin{pmatrix} 0.0 \\ 10401.526536 \\ 0.0 \end{pmatrix} \times 10^3 m/\sec \qquad (26)$$

Table 3: Case 2 Elliptical Orbit (E=0.2) Integration Performance & Accuracy Study: Continuation for 1 orbital period

# of Continuation Steps & Integration Step Size(sec) (Orbit Period = 8145.5912 sec)	# Series Terms for mm error /Final Integration accuracy
200, 40.7280	4 (10^{-8} m, 10^{-10} m/s)
100, 81.4559	5 (10^{-7} m, 10^{-10} m/s)
80, 101.8199	6 (10^{-8} m, 10^{-11} m/s)
60, 135.7599	6 (10^{-7} m, 10^{-10} m/s)
40, 203.6398	8 (10^{-7} m, 10^{-10} m/s)
3, 271.5197	8 (10^{-5} m, 10^{-8} m/s)
20, 407.2796	11 (10^{-2} m, 10^{-5} m/s)
15, 543.0394	15 (10^{1} m, 10^{-3} m/s)

The orbit eccentricity is 0.9. Table 4 shows sub-meter accuracy achieved for a step size of $\sim$ 184 sec. Only five derivative orders are required. Of course, this example needs to have step size control imposed because the only interesting motion is near perigee. Very large performance gains are possible and future research will investigate strategies for studying these problems. The high accuracy achieved for this application provides great confidence that asteroid motion prediction can be carried out to very high precision, and that the associated sensitivity partial derivative calculations for supporting the propagation of modeling uncertainty are computed with high accuracy.

5.4. Case 4: 700 km Altitude elliptical Earth Orbit

The initial position and velocity vectors are

$$r(t_0) = \begin{pmatrix} 1.8917122 \\ 3.7834254 \\ 5.6751367 \end{pmatrix} \times 10^6 m; \qquad \dot{r}(t_0) = \begin{pmatrix} 0.0 \\ 7.5042925 \\ 0.0 \end{pmatrix} \times 10^3 m/\sec \quad (27)$$

The orbit eccentricity is 0.534522. Full 3D motions are excited. As is shown in Table 5, sub-meter accuracy is achieved for a step size of $\sim$ 150 sec. As the
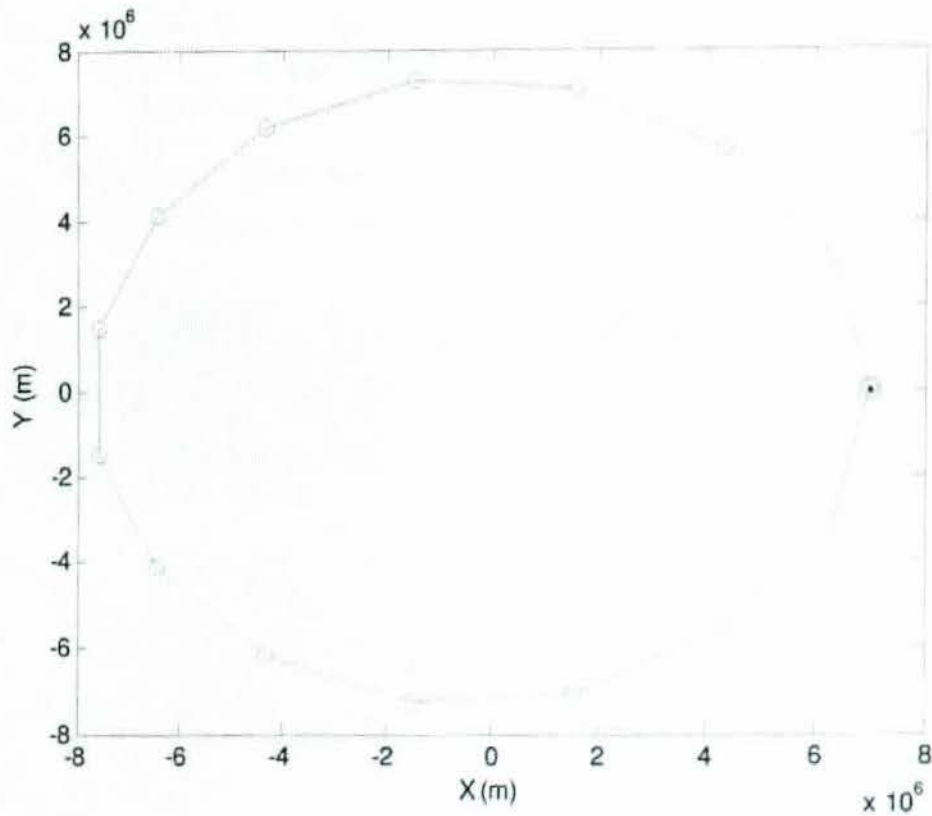
Figure 3: Continuation for 1 orbital period

Table 4: Case 3 Elliptical Orbit (E=0.9) Integration Performance & Accuracy Study: Continuation vs. F&G solution (2 weeks, 14 orbits)

# of Continuation Steps & Integration Step Size(sec) (Orbit Period = 184313 sec)	# Series Terms for mm error /Final Integration accuracy
5000, 36.8627	5 (10^{-5} m, 10^{-8} m/s)
3000, 61.4378	5 (10^{-5} m, 10^{-8} m/s)
1000, 184.3135	7 (10^{-2} m, 10^{-5} m/s)
800, 230.3919	10 (10^{1} m, 10^{-3} m/s)

integration step size approaches 100 sec. the solution accuracy is beyond double precision arithmetic (i.e., 14 digits) and only seven series terms are required.
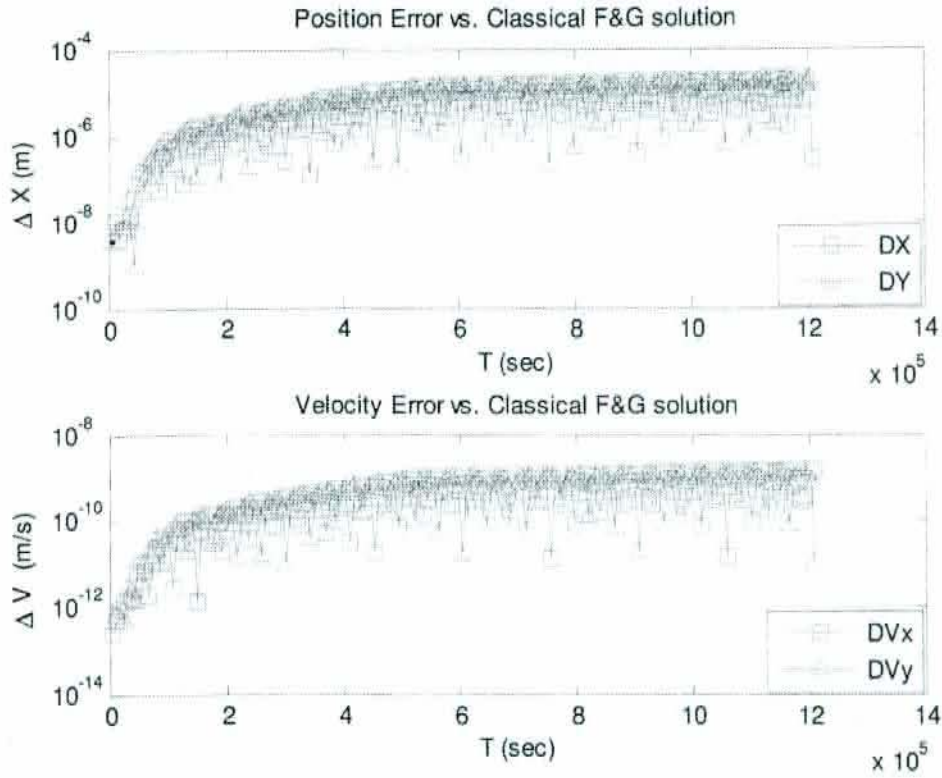
Figure 4: Continuation vs. F&G solution (2 weeks, 14 orbits)

Table 5: Case 4 Elliptical Orbit Integration Performance & Accuracy Study

# of Continuation Steps & Integration Step Size(sec)(Orbit Period = 5926.376 sec)	# Series Terms for mm error /Final Integration accuracy
200, 29.6319	6 (10^{-7} m, 10^{-10} m/s)
100, 59.2638	7 (10^{-6} m, 10^{-9} m/s)
80, 74.0797	8 (10^{-5} m, 10^{-8} m/s)
60, 98.7729	9 (10^{-2} m, 10^{-7} m/s)
40, 148.1594	10 (10^{-1} m, 10^{-4} m/s)
35, 169.3250	11 (10 m, 10^{-2} m/s)
30, 197.5459	12 (10^{-1} m, 10^{-1} m/s)
25, 237.0550	Failed to Converge

5.5. Case 5: 42241 km altitude Circular Earth Orbit (GEO)

The initial position and velocity vectors are

$$r(t_0) = \begin{pmatrix} 4.2241121 \\ 0.0 \\ 0.0 \end{pmatrix} \times 10^8 m; \qquad \dot{r}(t_0) = \begin{pmatrix} 0.0 \\ 3.0718612 \\ 0.0 \end{pmatrix} \times 10^3 m/\sec$$

The results of Table 6 indicate that Circular Orbits are easy to integrate compared to elliptical orbits. In deed the step sizes for the circular case are *3-5 X* larger than can be handled for elliptical cases. Generally 8-10 analytic continuation steps are required to achieve *mm* position error levels. Future research will investigate the impact of modeling these cases using an extended precision version of the software.

Table 6: Case 5 GEO Circular Orbit Integration Performance & Accuracy Study

# of Continuation Steps &Integration Step Size(sec)(Orbit Period = 86400 sec)	# Series Terms for mm error /Final Integration accuracy
60, 1439.999	6 (10^{-6} m, 10^{-10} m/s)
40, 2159.999	6 (10^{-6} m, 10^{-11} m/s)
35, 2468.571	7 (10^{-7} m, 10^{-11} m/s)
30, 2879.999	8 (10^{-6} m, 10^{-11} m/s)
25, 3455.999	8 (10^{-7} m, 10^{-11} m/s)
20, 4319.999	9 (10^{-7} m, 10^{-11} m/s)
15, 5759.999	10 (10^{-5} m, 10^{-9} m/s)
10, 8639.999	10 (10^{-2} m, 10^{-6} m/s)
5, 17279.999	14 (10^{-1} m, 10^{-2} m/s)

For this specific case the algorithm accuracy is tested versus the F&G classical solution for an extended time period. Instead of integrating for 1 orbital period the trajectory is generated for approximately 2 weeks, about 14 orbits. Figure 4 shows the errors in position & velocity at each time step vs. the F&G solution.

It is quite clear the consistency of the solution with the known closed form solution at each time step, where the accuracy is advanced at each time step over the whole

period of the trajectory generation. This consistency combined with the speed of convergence of the algorithm can have a significant impact on orbit determination and propagation techniques.

6. CONCLUSIONS AND FUTURE DIRECTIONS

A new algorithm is presented that computes arbitrary time derivatives of the two-body problem using a recursive formulation. The key paper contribution is the identification of Lagrange-like invariants that re-cast the two-body calculations in a product form that is handled by Leibniz product rule. Leibniz product rule is applied sequentially to both Lagrange-like invariants and the two-body equation of motion. Simulations have been successfully performed that included up to 40 exact time derivatives for the two-body motion. Several numerical trajectory calculations are presented that demonstrate that simple analytical continuation calculations produce high precision calculations for the both position and velocity vectors. Extensions are presented for evaluating the uncertainty of the initial conditions by developing a nonlinear state transition matrix series expansion. These equations are used to transform samples from the initial uncertainty covariance matrix to develop a transformation for modifying the underlying *pdf*. A reversion of series solution is presented for the state transition matrix series that effectively solves the *stochastic Liouville equation* for the *pdf* in presence of low diffusion effects. Numerical results are presented for studying the evolution of the *pdf* during a trajectory motion. Future research will extend the results in two ways: (1) extended precession calculations will be introduced for investigating the maximum integration step sizes that can be supported by the proposed analytic continuation modeling algorithm and (2) the state transition tensors will be developed as power series expansions for computational efficiency.

7. REFERENCES

[1] Lagrange, J. L., *Méchanique Analytique*, Pais, 1788.

[2] Hamilton, W. R., *On a General Method in Dynamics*, Collected Papers of W. R. Hamilton, Vol. II, Cambridge Univ. Press, 1940, pp. 103-211.

[3] Pars, L. A., *A Treatise on Analytical Dynamics*, Wiley, New York, 1965, Chaps. 22-25.

[4] Boruwer, D., and Clemence, G., *Methods of Celestial Mechanics*, Academic Press, New York, 1961, Chap. 17.

[5] Goldstein, H., *Classical Mechanics*, Addison-Wesley, 1950.

[6] Junkins, J. L. , and Turner, J. D., *Optimal Spacecraft Rotational Maneuvers*, Elsevier, Amsterdam, 1986.

[7] Schaub, H., and Junkins, J. L., *Analytical Mechanics of Space Systems Second Edition*, AIAA Education Series, Editor Joseph A. Schetz, 2009.

[8] Majji, M., Junkins, J. L., and Turner, J. D., Measurement Model Nonlinearity in Estimation of Dynamical Systems, Paper AAS 10-300, Presented at— *Kyle T. Alfriend Astrodynamics Symposium* , Monterey Plaza Hotel & Spa, Monterey, California, May 17-19, 2010.

[9] Bailey, D. H., Hida, Y., Li, X. S., and Thompson, B., *ARPREC: An Arbitrary Precision Computation Package*, U. S. Department of Energy, Office of Computational and Technology Research, under Contract Number DE-AC03-76SF00098, pp. 1-8.